Materials Chemistry and Physics 238 (2019) 121955

Contents lists available at ScienceDirect

Materials Chemistry and Physics

journal homepage: www.elsevier.com/locate/matchemphys

Thermal reactions of nitrocellulose-encapsulated Al/CuO nanoenergetic materials fabricated in the gas and liquid phases

Ji Hoon Kim [a], Jeong Keun Cha [b], Myung Hoon Cho [a], Hosung Kim [b], Hong-Min Shim [c], Soo Hyung Kim [a,b,d,*]

[a] *Research Center for Energy Convergence Technology, Pusan National University, 2, Busandaehak-ro 63 beon-gil, Geumjeong-gu, Busan, 46241, Republic of Korea*
[b] *Department of Nano Fusion Technology, College of Nanoscience and Nanotechnology, Pusan National University, 2, Busandaehak-ro 63 beon-gil, Geumjeong-gu, Busan, 46241, Republic of Korea*
[c] *Agency for Defense Development, P.O. Box 35, Yuseong, Daejeon, 34186, Republic of Korea*
[d] *Department of Nanoenergy Engineering, College of Nanoscience and Nanotechnology, Pusan National University, 2, Busandaehak-ro 63beon-gil, Geumjeong-gu, Busan, 46241, Republic of Korea*

HIGHLIGHTS

- Al–CuO–nitrocellulose composite is fabricated by aerosol drying process (ADP).
- NC content strongly affects redox reactivity and electrical insensitivity.
- ADP provides high-performance nanoscale energetic materials with homogeneous component mixing.

ARTICLE INFO

Keywords:
Polymer encapsulation
Energetic materials
Nitrocellulose
Aerosol drying process
Insensitivity

ABSTRACT

We examined the effect of polymer encapsulation on the insensitivity and thermal reactions of Al and CuO-based nanoenergetic materials (nEMs). The nEMs were encapsulated by nitrocellulose (NC) polymer using aerosol and solution drying processes for comparison. Severe aggregation and precipitation of Al/CuO reactants in the NC matrix were made in the liquid phase during the drying process so that the thermal reactions of the resulting Al/CuO/NC composites was unstable. However, the rapid aerosol drying process in the gas phase resulted in the formation of uniformly mixed NC-encapsulated Al/CuO composites. The NC content in the Al/CuO composites fabricated in the gas phase strongly affected the thermal reactions by perturbing thermochemical interactions between the Al and CuO reactants. Meanwhile, the insensitivity of Al/CuO composites gradually increased with increasing NC content. Therefore, the aerosol drying process in the gas phase is suggested as a viable and effective method to generate polymer-encapsulated homogeneously mixed nEMs with enhanced insensitivity and thermal reaction properties.

1. Introduction

Nanoenergetic materials (nEMs) are substances comprising nanoscale fuels (e.g., Al, Si, Mg) and oxidizers (e.g., CuO, Fe_2O_3, NiO), which rapidly generate exothermic energy when ignition is initiated [1–12]. However, owing to the high sensitivity to the external stimuli such as electrostatic discharge, shock, and friction, the practical applications of nEMs have been limited [13]. Therefore, numerous researches have been conducted to improve the insensitivity of nEMs by incorporating with CNT [14,15], graphene [14], carbon black [16] and carbon nanofiber [17], or polymers [18,19].

Recently, various polymers are widely applied to nEMs not only as an insensitizer but also as binders [6,20], hydrophobic coating agents [20,21], surface passivation agents [22–24], and functionalization mediums [25]. However, conventional physical mixing processes are inherently limited for uniformly dispersing nEMs in polymer binders because the relatively long drying and curing processes for polymer binders induce the aggregation and precipitation of nEMs with high-surface-energy [26,

* Corresponding author. Research Center for Energy Convergence Technology, Pusan National University, 2, Busandaehak-ro 63beon-gil, Geumjeong-gu, Busan, 46241, Republic of Korea.
E-mail address: sookim@pusan.ac.kr (S.H. Kim).

https://doi.org/10.1016/j.matchemphys.2019.121955
Received 4 May 2019; Received in revised form 23 July 2019; Accepted 4 August 2019
Available online 5 August 2019

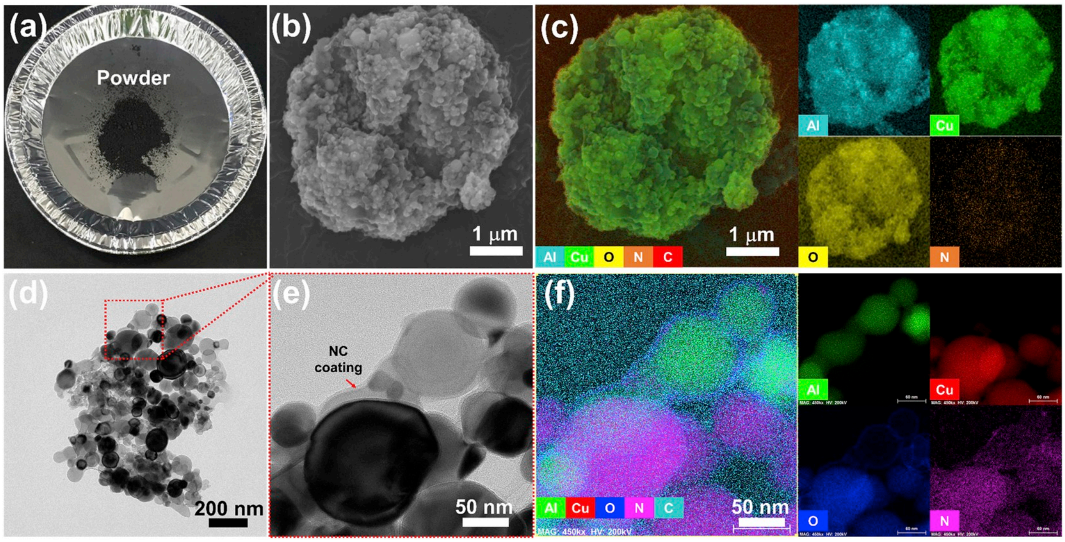

Fig. 1. (a) Photograph, (b) SEM, (c) EDS, (d) LRTEM, (e) HRTEM, and (f) EDS images of NC-encapsulated Al/CuO composites fabricated by ADP.

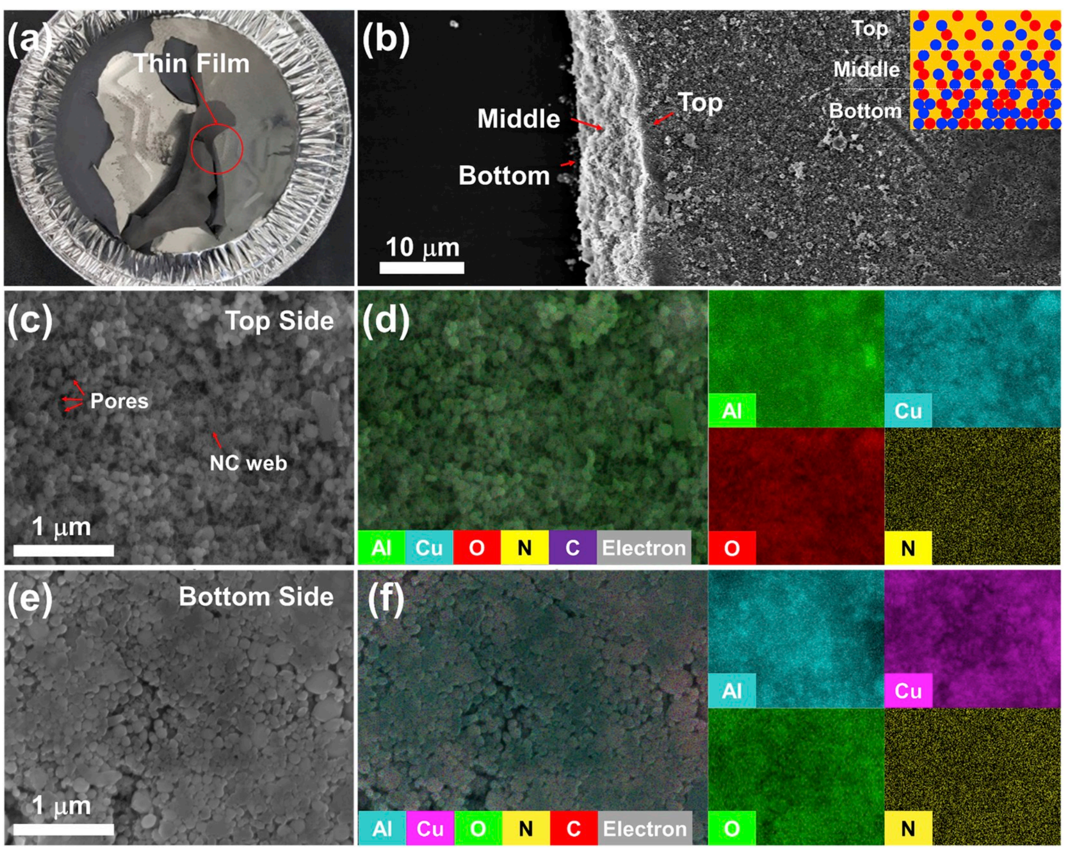

Fig. 2. (a) Photograph, SEM & EDS images of (b) entire, (c, d) top, and (e, f) bottom side of Al/CuO/NC composite thin film fabricated by SDP.

27]. These problems finally result in the significant degradation of combustion characteristics of nEM-polymer composites.

To fabricate uniform nEM-polymer composites, electrospray and electrospinning processes in the gas phase are often employed with the advantages of production of uniform particles and capability of aerosolization of precursor solution with relatively high viscosity [28–32]. However, the potential risk of unintended explosion exists due to the supply of high voltage in the electrostatic charging process, and simultaneously the relatively low yield rate of the resulting composites is the major inherent bottleneck.

To overcome these difficulties, we propose an easy and viable gas-phase aerosol synthesis of polymer-encapsulated nEMs, which have relatively high insensitivity and homogeneous mixtures. Briefly, nitrocellulose (NC), Al nanoparticles (NP), and CuO NPs are used as the polymer binder, fuel metal, and oxidizer, respectively. NC is employed as an energetic polymer binder that functions as both an abundant exothermic energy source and a gas generator during the combustion of nEMs. In the present study, an aerosol drying process (ADP) [33–35] is

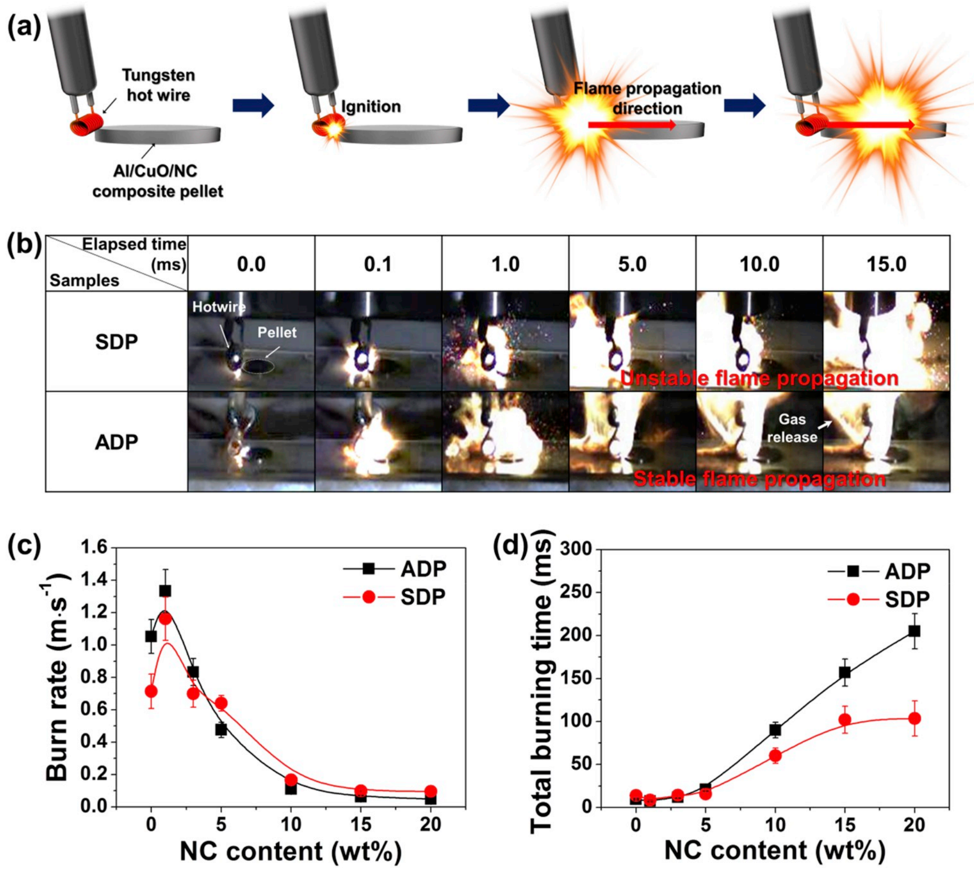

Fig. 3. (a) Schematic and (b) snapshots of ignition and combustion of Al/CuO/NC (20 wt%) composite pellets NC fabricated by SDP and ADP. (c) Burn rates and (d) total burning times of Al/CuO/NC composite pellets with various NC contents.

employed to fabricate NC-encapsulated Al/CuO composite particles through the rapid drying of the aerosolized precursor solution. Various parameters, including NC concentration and drying conditions, are systematically examined to explore the insensitivity and thermal reactions of the resulting NC-coated nEMs (i.e., Al/CuO NPs).

2. Experimental

Al and CuO NPs (Nanotechnology Co., Ltd.) and NC (Sigma-Aldrich) were used as raw materials. The Al and CuO NPs were mixed with a mass ratio of Al:CuO = 3:7 (i.e., fuel-to-oxidizer ratio = 1.90) as the optimized combustion properties [36] in an ethanol/ether solution using ultrasonic mixing (400 W, 40 kHz) for 1 h. Subsequently, NC solutions with various initial concentrations of 1, 2, 5, 10, 15, and 20 wt% were then mixed with the fabricated Al/CuO NP colloidal solutions. For ADP, the resulting precursor solution was transferred using a peristaltic pump to a nozzle operated at 7 MPa to aerosolize the Al/CuO/NC precursor solution. The generated Al/CuO/NC droplets were rapidly solidified by solvent evaporation driven by the hot carrier gas, thereby forming composite particles. For comparison, Al/CuO/NC composites were also fabricated using a conventional solution drying process (SDP), in which the Al/CuO/NC solution was poured into a dish and dried for 24 h at 20 °C. The Al/CuO/NC composites were characterized using various techniques, including a field emission scanning electron microscope (FE-SEM, Carl Zeiss, Supra 25, Germany) operated at ~20 kV equipped with an energy dispersive X-ray analyzer (EDS, Oxford Instruments, INCA, UK), scanning transmission electron microscopy (STEM; FEI, Talos F200X) performed at ~200 kV, and differential scanning calorimetry (DSC; Setaram, Ltd., Labsys evo) performed at temperatures of 30–1000 °C at a heating rate of 10 °C min^{-1} under Ar flow. For thermal ignition tests, the Al/CuO/NC composites were formed into disk-type pellets by die-compaction process. Briefly, 100 mg of composites was poured into a mold and pelletized into a disk with a diameter of 10 mm and a height of ~0.4 mm under a pressure of 300 MPa. The burn rate and total burning time of the Al/CuO/NC composite pellets were measured using a high-speed camera (Photron, FASTCAM SA3 120 K) at a frame rate of 50 kHz. The pressure traces of the composites ignited in a closed vessel were measured using a pressure cell tester (PCT) system. It was conducted by placing 13 mg of the tested powder in the sealed pressure cell and igniting it with a hot tungsten wire at a current of 2 A and voltage of 4 V. The explosion pressure was measured using a piezoelectric pressure sensor (113A03, PCB Piezotronics) attached to the pressure cell. Simultaneously, the detected pressure signal was amplified and transformed into a voltage signal through a combination of an in-line charge amplifier (422E11, PCB Piezotronics) and signal conditioner (480C02, PCB Piezotronics). Finally, the signal was captured and recorded using a digital oscilloscope (TDS 2012B, Tektronix). The electrostatic discharge (ESD) sensitivities of the composites were measured using an ESD simulator (Kikuchi, KES4021). The electrical energy stored in the 150 pF capacitor with a specific voltage (0–30 kV) was instantaneously discharged through a cylindrical wire-type electrode to artificially generate an electric spark. The spark energy was calculated by formula $E = 0.5\ CV^2$, where C is the capacitance of the capacitor in farads (F) and V is the voltage in volts (V). The distance between the grounded sample stage and spark tip was fixed to ~2 mm. The ignition threshold spark energy (ITSE) was determined using the "go/no go" method. If ignition and successive explosion occurred at specific spark energy, lower spark energy was selected as the ITSE for the tested sample. Each kind of sample was tested ~10 times repeatedly. The density of the sample powder was 11–17% of theoretical maximum density (%TMD) and the relative humidity during testing was fixed to ~30%.

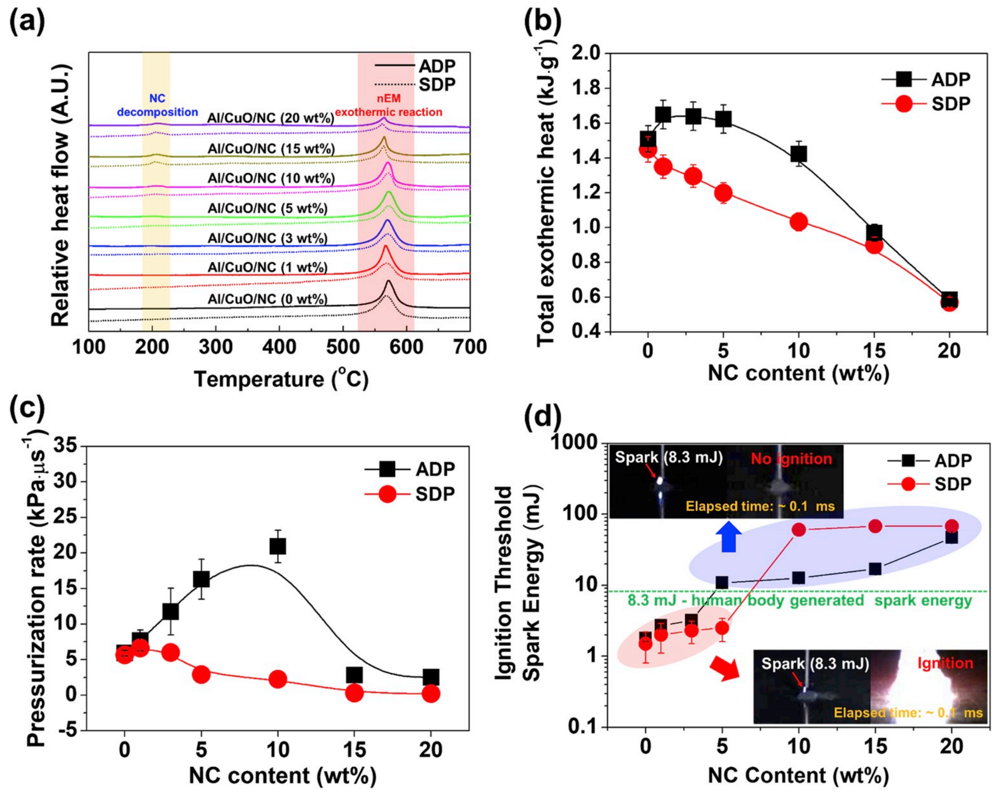

Fig. 4. (a) DSC results, (b) total exothermic heats, and (c) pressurization rates of Al/CuO/NC composites fabricated by ADP and SDP. (d) ITSE of NC-encapsulated Al/CuO composites with various NC contents fabricated by ADP and SDP (Insets: Still images of spark ignition tests for NC-encapsulated Al/CuO composites fabricated by ADP).

3. Results and discussion

Fig. 1a–f shows photographic, SEM, low-resolution TEM (LRTEM), high-resolution TEM (HRTEM), and energy-dispersive X-ray spectroscopy (EDS) images, respectively, of the Al/CuO/NC composite particles with 10 wt% NC fabricated by ADP. SEM and TEM images present that Al and CuO NPs with an average diameter of ~80 nm are strongly bound and encapsulated by thin layers of NC. The EDS images reveal that Al and CuO NPs were homogeneously distributed in the composite particles.

The Al/CuO/NC composite fabricated by SDP was formed into a thin film of ~10 μm in thickness, as shown in Fig. 2a–f. The SEM analyses for the thin film formed show that various pores and NC webs were formed on the top side, and denser particle clusters were formed in the bottom side. The SEM and EDS analyses confirmed that Al and CuO NPs were precipitated in the bottom of NC matrix. This suggests that Al and CuO NPs were found to be non-homogeneously distributed in the depth direction because of the aggregation and precipitation of Al and CuO NPs under SDP.

Thermal ignition tests were performed to examine the effect of NC encapsulation on the thermal reactions of the ADP-fabricated Al/CuO composites. For thermal ignition testing, the composites were formed into disk-type pellets and ignited by a tungsten hotwire igniter (Fig. 3a). The densities of composite pellets were calculated to be ~79–96 %TMD and ~71–82 %TMD for the cases of ADP and SDP, respectively (see Fig. S1 in the Supporting Information). The ADP-fabricated pellet had higher density due to more homogeneous mixing of NC polymer and Al/CuO NPs. And the differences in mixing states of composite pellets fabricated by both ADP and SDP seemed to strongly affect the flame propagation of the ignited composite pellets. Fig. 3b shows the sequential still images of the ignition and flame propagation of Al/CuO/NC (20 wt%) composite pellets fabricated by ADP and SDP, respectively, captured using a high-speed camera. For ADP-fabricated NC (20 wt%)-encapsulated Al/CuO composite pellet, considerable amount of combustion gases was generated with stable flame propagation. However, for the case of SDP-fabricated Al/CuO/NC (20 wt%) composite pellet, unstable flame propagation was occurred due to the non-uniform component mixing. Fig. 3c and d shows the burn rates and total burning times of Al/CuO/NC composites with various NC contents, as determined by high-speed camera snapshot analyses (see Fig. S2 in the Supporting Information). The burn rate decreased and the total burning time increased for increasing NC content. This was because the diffusion distance between the Al and CuO NPs increased by the greater thickness of the NC coating layer, which eventually suppressed the redox and thermochemical reactivity of the Al and CuO NPs.

Fig. 4a and b shows the DSC data and total exothermic heat energies of the composites fabricated by ADP and SDP. Two major exothermic peaks, attributed to the thermal decomposition of NC at ~170–230 °C and the redox reaction between Al and CuO NPs at 520–610 °C, were clearly observed (Fig. 4a). The resulting total exothermic heats of the Al/CuO/NC composites were determined by integrating both peaks (Fig. 4b). Overall, the total exothermic heat was decreased with increasing NC content because of the increasing diffusion distance between the Al and CuO NPs. In addition, the gas byproducts of thermal decomposition of NC (e.g., CO, CO_2, NO, etc.) could oxidize Al NPs to some extent, which resulted in reducing the heat release from the Al/CuO redox reaction occurred at 520–610 °C. We also observed that the total exothermic heat for ADP-fabricated composites with NC content of 1–5 wt% slightly increased. This was presumably because the gases generated by thermal decomposition of NC disintegrated Al/CuO composites so that they actively made redox reactions later in the combustion process [18]. The ADP-fabricated composites generated greater total exothermic heat than the SDP-fabricated composites because of the component homogeneity. Fig. 4c shows the pressurization rates of the Al/CuO/NC composites measured using the PCT system. The pressurization rates were determined by dividing the maximum pressures by the

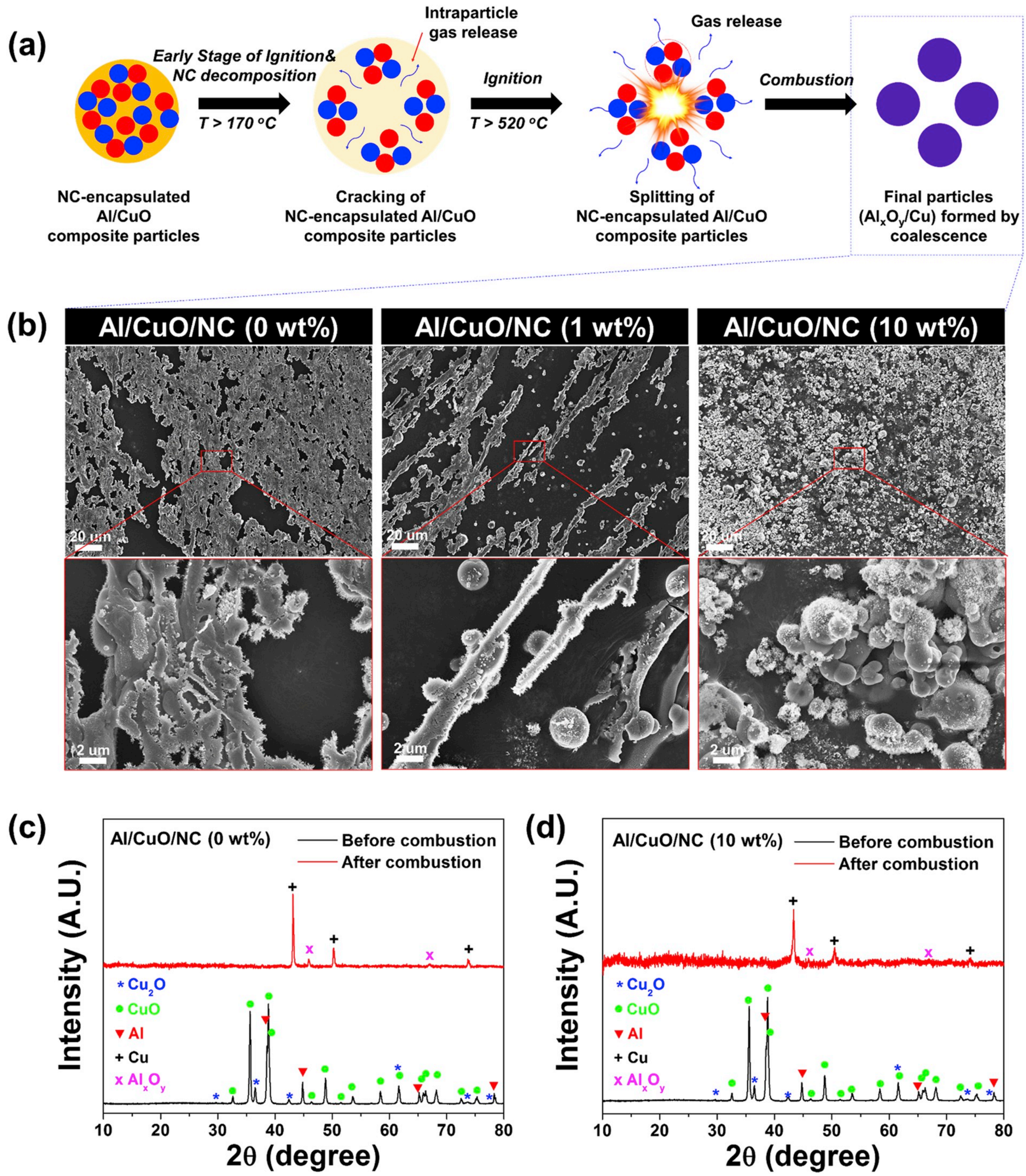

Fig. 5. (a) Schematic of thermal reactions of NC-encapsulated Al/CuO composite particles, (b) SEM images of NC-encapsulated Al/CuO composite particles with NC contents of 0, 1, and 10 wt% after combustion. XRD patterns of Al/CuO composite particles with NC content of (b) 0 wt% and (c) 10 wt% before and after combustion.

pressure rise times. For ADP composites, the pressurization rate was gradually increased with increasing NC content up to 10 wt%, because considerable combustion gases were generated by the thermal decomposition of NC [37]. However, for excessive NC contents of >15 wt% added to Al/CuO, the pressurization rate was significantly decreased because the increased diffusion distance between Al and CuO decreased the redox reactivity. For SDP composites, the pressurization rate was gradually decreased by increasing the NC content because of the inhomogeneous mixture formation in the Al/CuO/NC composites. Fig. 4d shows the ESD sensitivities of the NC-encapsulated Al/CuO composites fabricated by ADP and SDP. As the NC content increased, the ignition threshold spark energy (ITSE) increased because of the increased electrical resistivity of the NC-encapsulated Al/CuO composites [14,19]. For NC contents of >5 wt%, the ITSE value of ADP-fabricated samples was more than ~10 mJ, exceeding the spark energy generally generated by human body activity (~8.3 mJ) [38]. This suggests that the insensitivity of Al/CuO composites for practical applications can be sufficiently increased by NC polymer encapsulation via ADP. However, the Al/CuO/NC composites fabricated by SDP showed lower ITSE than ADP at NC contents of ≤5 wt% due to non-uniform NC coating. The ITSE was then abruptly increased at NC contents of ≥10 wt%, and the ignition did not occur even at the possible maximum spark energy of ~67.5 mJ in the ESD system. This suggests that the SDP-fabricated thick NC layer protected the surface of Al/CuO composite thin film from electric spark energy input when sufficient amount of NC contents (≥10 wt%) was provided.

Based on these experimental observations, we propose the following thermal reaction mechanism depicted in Fig. 5a. When the NC-encapsulated Al/CuO composites were heated, the thermal decomposition of NC began at ~170 °C. The Al/CuO/NC composite matrix then swelled with the combustion gas generated by NC thermal decomposition, causing cracking. When the temperature was further increased above ~520 °C, the Al/CuO composites experienced rapid redox reactions. Cracked composite particles with Al_xO_y and Cu intermediates were generated by the coalescence of Al/CuO composites with higher NC contents. SEM and X-ray diffraction (XRD) analyses for residual particles after combustion reactions, as shown in Fig. 5b–d, clearly showed that composite particles with Al_xO_y and Cu intermediates and significant cracking were generated by the coalescence of Al/CuO composites with higher NC contents.

4. Conclusions

We investigated the thermal reactions and insensitivity of NC-encapsulated Al/CuO composites fabricated using ADP. The NC-encapsulated Al/CuO composites fabricated by ADP had homogeneous mixtures of the Al/CuO/NC components that yielded much better resulting thermal reactions, including burn rate, pressurization rate, and exothermic heat energy, than those of composites fabricated by conventional SDP. In addition, the ESD insensitivity of the composites fabricated by ADP significantly increased with increasing NC content in the Al/CuO composites because of the increased NC coating layer thickness. The ADP method proposed in this study allows an easy, viable, and stable fabrication of nEMs with enhanced thermal reactions and insensitivity.

Acknowledgments

This research was financially supported by the Agency for Defense Development funded by the Defense Acquisition Program Administration (grant No. UD170034GD), South Korea. This study was also supported by the 2018 Post-Doc. Development Program of Pusan National University.

Appendix A. Supplementary data

Supplementary data to this article can be found online at https://doi.org/10.1016/j.matchemphys.2019.121955.

References

[1] S.H. Kim, M.R. Zachariah, Enhancing the rate of energy release from nanoenergetic materials by electrostatically enhanced assembly, Adv. Mater. 16 (2004) 1821–1825.
[2] K. Zhang, C. Rossi, P. Alphonse, C. Tenailleau, S. Cayez, J.-Y. Chane-Ching, Integrating Al with NiO nano honeycomb to realize an energetic material on silicon substrate, Appl. Phys. A 94 (2009) 957–962.
[3] S. Pourmortazavi, S. Hajimirsadeghi, I. Kohsari, M. Fathollahi, S. Hosseini, Thermal decomposition of pyrotechnic mixtures containing either aluminum or magnesium powder as fuel, Fuel 87 (2008) 244–251.
[4] M.S. Shin, J.K. Kim, J.W. Kim, C.A.M. Moraes, H.S. Kim, K.K. Koo, Reaction characteristics of Al/Fe_2O_3 nanocomposites, J. Ind. Eng. Chem. 18 (2012) 1768–1773.
[5] J.Z. Wen, S. Ringuette, G. Bohlouli-Zanjani, A. Hu, N.H. Nguyen, J. Persic, C. F. Petre, Y.N. Zhou, Characterization of thermochemical properties of Al nanoparticle and NiO nanowire composites, Nanoscale Res. Lett. 8 (2013) 184.
[6] X. Li, H. Yang, Y.C. Li, Characterization of thermal reaction of aluminum/copper (II) oxide/poly (tetrafluoroethene) nanocomposite by thermogravimetric analysis, differential scanning calorimetry, mass spectrometry and X-ray diffraction, Thermochim. Acta 621 (2015) 68–73.
[7] J. Shen, Z. Qiao, J. Wang, G. Yang, J. Chen, Z. Li, X. Liao, H. Wang, M.R. Zachariah, Reaction mechanism of Al-CuO nanothermites with addition of multilayer graphene, Thermochim. Acta 666 (2018) 60–65.
[8] S.G. Hosseini, A. Sheikhpour, M.H. Keshavarz, S. Tavangar, The effect of metal oxide particle size on the thermal behavior and ignition kinetic of Mg–CuO thermite mixture, Thermochim. Acta 626 (2016) 1–8.
[9] X. Zhou, Y. Wang, Z. Cheng, X. Ke, W. Jiang, Facile preparation and energetic characteristics of core-shell Al/CuO metastable intermolecular composite thin film on a silicon substrate, Chem. Eng. J. 328 (2017) 585–590.
[10] H.S. Kim, J.H. Kim, K.J. Kim, S.H. Kim, Tuning the ignition and combustion properties of nanoenergetic materials by incorporating with carbon black nanoparticles, Combust. Flame 194 (2018) 264–270.
[11] J.Y. Lyu, S. Chen, W. He, X.X. Zhang, D.Y. Tang, P.J. Liu, Q.L. Yan, Fabrication of high-performance graphene oxide doped PVDF/CuO/Al nanocomposites via electrospinning, Chem. Eng. J. 368 (2019) 129–137.
[12] C. Rossi, Engineering of Al/CuO reactive multilayer thin films for tunable initiation and actuation, Propellants, Explos. Pyrotech. 44 (2019) 94–108.
[13] D.G. Piercey, T.M. Klapoetke, Nanoscale aluminum-metal oxide (thermite) reactions for application in energetic materials, Cent. Eur. J. Energetic Mater. 7 (2010) 115–129.
[14] E.S. Collins, B.R. Skelton, M.L. Pantoya, F. Irin, M.J. Green, M.A. Daniels, Ignition sensitivity and electrical conductivity of an aluminum fluoropolymer reactive material with carbon nanofillers, Combust. Flame 162 (2015) 1417–1421.
[15] K.H. Poper, E.S. Collins, M.L. Pantoya, M.A. Daniels, Controlling the electrostatic discharge ignition sensitivity of composite energetic materials using carbon nanotube additives, J. Electrost. 72 (2014) 428–432.
[16] A. Bach, P. Gibot, L. Vidal, R. Gadiou, D. Spitzer, Modulation of the reactivity of a WO_3/Al energetic material with graphitized carbon black as additive, J. Energetic Mater. 33 (2015) 260–276.
[17] B. Siegert, M. Comet, O. Muller, G. Pourroy, D. Spitzer, Reduced-sensitivity nanothermites containing manganese oxide filled carbon nanofibers, J. Phys. Chem. C 114 (2010) 19562–19568.
[18] J. Dai, J. Xu, F. Wang, Y. Tai, Y. Shen, R. Shen, Y. Ye, Facile formation of nitrocellulose-coated Al/Bi_2O_3 nanothermites with excellent energy output and improved electrostatic discharge safety, Mater. Des. 143 (2018) 93–103.
[19] T. Foley, A. Pacheco, J. Malchi, R. Yetter, K. Higa, Development of nanothermite composites with variable electrostatic discharge ignition thresholds, Propellants, Explos. Pyrotech. 32 (2007) 431–434.
[20] K.J. Kim, M.H. Cho, J.H. Kim, S.H. Kim, Effect of paraffin wax on combustion properties and surface protection of Al/CuO-based nanoenergetic composite pellets, Combust. Flame 198 (2018) 169–175.
[21] J.H. Kim, S.B. Kim, M.G. Choi, D.H. Kim, K.T. Kim, H.M. Lee, H.W. Lee, J.M. Kim, S.H. Kim, Flash-ignitable nanoenergetic materials with tunable underwater explosion reactivity: the role of sea urchin-like carbon nanotubes, Combust. Flame 162 (2015) 1448–1454.
[22] D.W. Kim, K.T. Kim, T.S. Min, K.J. Kim, S.H. Kim, Improved energetic-behaviors of spontaneously surface-mediated Al particles, Sci. Rep. 7 (2017) 4659.
[23] J. Wang, A. Hu, J. Persic, J.Z. Wen, Y.N. Zhou, Thermal stability and reaction properties of passivated Al/CuO nano-thermite, J. Phys. Chem. Solids 72 (2011) 620–625.
[24] R.J. Jouet, A.D. Warren, D.M. Rosenberg, V.J. Bellitto, K. Park, M.R. Zachariah, Surface passivation of bare aluminum nanoparticles using perfluoroalkyl carboxylic acids, Chem. Mater. 17 (2005) 2987–2996.
[25] K.S. Kappagantula, C. Farley, M.L. Pantoya, J. Horn, Tuning energetic material reactivity using surface functionalization of aluminum fuels, J. Phys. Chem. C 116 (2012) 24469–24475.
[26] M.E. Mackay, A. Tuteja, P.M. Duxbury, C.J. Hawker, B. Van Horn, Z. Guan, C. Guanghui, R.S. Krishnan, General strategies for nanoparticle dispersion, Science 311 (2006) 1740–1743.
[27] J. Liu, Y. Gao, D. Cao, L. Zhang, Z. Guo, Nanoparticle dispersion and aggregation in polymer nanocomposites: insights from molecular dynamics simulation, Langmuir 27 (2011) 7926–7933.
[28] X. Zhang, B.L. Weeks, Preparation of sub-micron nitrocellulose particles for improved combustion behavior, J. Hazard Mater. 268 (2014) 224–228.
[29] K.K. Kuo, Fundamentals of Solid-Propellant Combustion, American Institute of Aeronautics and Astronautics, 1984.
[30] H. Wang, G. Jian, W. Zhou, J. DeLisio, V. Lee, M. Zachariah, Metal iodate-based energetic composites and their combustion and biocidal performance, ACS Appl. Mater. Interfaces 7 (2015) 17363–17370.
[31] S. Yan, G. Jian, M.R. Zachariah, Electrospun nanofiber-based thermite textiles and their reactive properties, ACS Appl. Mater. Interfaces 4 (2012) 6432–6435.
[32] B.K. Ku, S.S. Kim, Electrospray characteristics of highly viscous liquids, J. Aerosol Sci. 33 (2002) 1361–1378.
[33] A. Gharsallaoui, G. Roudaut, O. Chambin, A. Voilley, R. Saurel, Applications of spray-drying in microencapsulation of food ingredients: an overview, Food Res. Int. 40 (2007) 1107–1121.
[34] R. Vehring, Pharmaceutical particle engineering via spray drying, Pharm. Res. 25 (2008) 999–1022.
[35] T.T.T. Kodas, M.J. Hampden-Smith, Aerosol Processing of Materials, Wiley-Vch, 1999.
[36] J.Y. Ahn, W.D. Kim, K. Cho, D. Lee, S.H. Kim, Effect of metal oxide nanostructures on the explosive property of metastable intermolecular composite particles, Powder Technol. 211 (2011) 65–71.
[37] M. Jin, N. Luo, G. Li, Y. Luo, The thermal decomposition mechanism of nitrocellulose aerogel, J. Therm. Anal. Calorim. 121 (2015) 901–908.
[38] W.D. Greason, Electrostatic discharge characteristics for the human body and circuit packs, J. Electrost. 59 (2003) 285–300.